

**F/6 21/5**

A PRIMITIVE VARIABLE COMPUTER MODEL FOR COMBUSTION WITHIN SOLID--ETC(

OCT 79 C A STEVENSON, D W NETZER

UNCLASSIFIED NP567-79-010

NL

1 OF 1  
AD  
2018-07-11

AD  
ADH-021

END

DATE \_\_\_\_\_

FINED

2

çifti

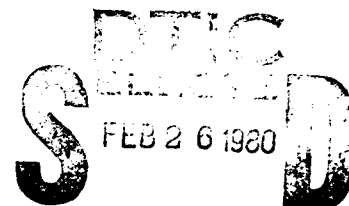
NPS67-79-010

EV # 2

# NAVAL POSTGRADUATE SCHOOL

Monterey, California

DA081081



A

A PRIMITIVE VARIABLE COMPUTER MODEL FOR  
COMBUSTION WITHIN SOLID FUEL RAMJETS

Charles A. Stevenson and David W. Netzer

October 1979

Approved for public release; distribution unlimited

Prepared for:

Naval Weapons Center  
China Lake, Ca

DDC FILE COPY

80 2 19 115

NAVAL POSTGRADUATE SCHOOL  
Monterey, California

Rear Admiral T. F. Dedman  
Superintendent

Jack R. Borsting  
Provost

The work reported herein was supported by the Naval Weapons Center,  
China Lake, CA.

Reproduction of all or part of this report is authorized.

This report was prepared by:



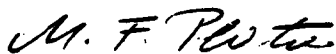
CHARLES A. STEVENSON  
LT, USN



DAVID W. NETZER  
Associate Professor of Aeronautics

Reviewed by:

Released by:



M. F. PLATZER, Chairman  
Department of Aeronautics



W. M. TOLLES  
Dean of Research

REPORT DOCUMENTATION PAGE		READ INSTRUCTIONS BEFORE COMPLETING FORM
1. REPORT NUMBER 14 NPS67-79-010	2. GOVT ACCESSION NO.	3. RECIPIENT'S CATALOG NUMBER 9
4. TITLE (and Subtitle) 6 A Primitive Variable Computer Model for Combustion Within Solid Fuel Ramjets		5. DATE OF REPORT & PERIOD COVERED Final 1979
7. AUTHOR(s) 10 Charles A. Stevenson Associate Professor/David W. Netzer		8. CONTRACT OR GRANT NUMBER(s) 12 45
9. PERFORMING ORGANIZATION NAME AND ADDRESS Naval Postgraduate School Code 67Nt Monterey, CA 93940		10. PROGRAM ELEMENT, PROJECT, TASK AREA & WORK UNIT NUMBERS N6053079WR30045
11. CONTROLLING OFFICE NAME AND ADDRESS Naval Weapons Center, China Lake, CA		12. REPORT DATE 14 October 1979
14. MONITORING AGENCY NAME & ADDRESS (if different from Controlling Office)		13. NUMBER OF PAGES 36
		15. SECURITY CLASS. (of this report) Unclassified
		16a. DECLASSIFICATION/DOWNGRADING SCHEDULE
16. DISTRIBUTION STATEMENT (of this Report)		
17. DISTRIBUTION STATEMENT (of the abstract entered in Block 20, if different from Report) Approved for public release; distribution unlimited		
18. SUPPLEMENTARY NOTES		
19. KEY WORDS (Continue on reverse side if necessary and identify by block number) Solid Fuel Ramjet Computer Model		
20. ABSTRACT (Continue on reverse side if necessary and identify by block number) An adaptation of a primitive variable, finite-difference computer program was accomplished in order to predict the reacting flow field in a solid fuel ramjet. The study compares the predictions of the primitive variable computer model with an earlier computer model and empirical data. It was found that the new model reasonably predicted the flow field and permitted calculations within the aft mixing chamber.		

DD FORM 1473  
1 JAN 73EDITION OF 1 NOV 66 IS OBSOLETE  
S/N 0102-014-6601

SECURITY CLASSIFICATION OF THIS PAGE (When Data Entered)

25145

JLC

## TABLE OF CONTENTS

I.	INTRODUCTION -----	1
II.	MODEL OVERVIEW -----	4
	A. INTRODUCTION -----	4
	B. ASSUMPTIONS -----	4
	C. GOVERNING EQUATIONS -----	6
	D. CONSERVATION OF MASS -----	9
	E. BOUNDARY CONDITIONS -----	10
	F. SOLUTION PROCEDURE -----	15
III.	DISCUSSION OF RESULTS -----	16
	A. INTRODUCTION -----	16
	B. REGRESSION RATE -----	17
	C. TURBULENCE INTENSITY -----	18
	D. PRESSURE -----	19
	E. TEMPERATURE -----	19
	F. COMPUTER RELATED PROBLEMS -----	23
IV.	CONCLUSIONS -----	24
V.	REFERENCES -----	35

Accession for	
NTIS Grant	<input checked="checked" type="checkbox"/>
DDC TAB	<input type="checkbox"/>
Unannounced	<input type="checkbox"/>
Justification	
By _____	
Distribution/	
Availability Codes	
Not	Available and/or special
A	

## ABBREVIATIONS AND SYMBOLS

### ROMAN SYMBOLS

A	Area
BP	Mass transfer (or "blowing") parameter
$C_1$	K-ε model empirical constants (Table I)
$C_2$	
$C_D$	
$C_f$	Coefficient of friction
$C_p$	Specific heat at constant pressure
E	9.0
g	Mass transfer conductance
G	Air mass flux
gr	Gram
h	Enthalpy
$\tilde{h}$	Stagnation enthalpy
H	Dimensionless enthalpy
$h$	Heat transfer conductance
i	Stoichiometric coefficient
I	Turbulence intensity
K, k	Turbulence kinetic energy
$\tilde{K}$	Thermal conductivity
l	Length Scale of turbulence
m	Mass fraction
M	Molecular weight

$\bar{M}$	Average molecular weight
$\dot{m}$	Mass flow rate
$\dot{m}''$	Mass flux
$P, p$	Pressure
$\dot{q}''$	Heat flux
$r$	Radial distance
$R$	Gas constant
$\bar{R}$	Universal gas constant
$RR, \dot{r}$	Regression rate
$S$	Source terms
$St$	Stanton number
$T$	Temperature
$u$	Axial velocity
$v$	Radial velocity
$x$	Axial distance
$y_p^+$	Dimensionless distance from solid boundary

#### GREEK SYMBOLS

$\Gamma$	Effective transport coefficient
$\delta$	Incremental distance from wall
$\Delta H$	Heat of combustion per Kg of fuel
$\epsilon$	Turbulence dissipation rate
$\kappa$	von Karman constant
$\mu$	Viscosity
$\rho$	Density

$\sigma$	Prandtl or Schmidt Number
$\tau$	Shear stress
$\phi$	Any variable
$X$	$m_{fu} - m_{ox}/i$

#### SUBSCRIPTS

air	Air
atm	Atmosphere
bw	Fuel surface (or "blowing wall")
c	Conserved
eff	Effective
fg	Fuel grain
fp	Fuel port
fu	Fuel
in	Inlet
lam	Laminar
N2	Nitrogen
ox	Oxygen
p	Near wall node
pr	Products
ref	Reference
t	Turbulent
T	Total
w	Wall



LIST OF TABLES

I.	K- $\epsilon$ Turbulence Model Empirical Constants	-----	5
II.	Governing Equation Parameters	-----	7
III.	Solid Fuel Ramjet Test Conditions	-----	20

## LIST OF FIGURES

1. Solid Fuel Ramjet Geometry and Boundary Conditions -----	25
2. Plexiglass Regression Rates -----	26
3. Effects of Air Mass Flux on the Predicted Regression Rates of the Primitive Variable Computer Model -----	27
4. Centerline Turbulence Intensity -----	28
5. Predicted Centerline Turbulence Intensity as a Function of Inlet Velocity (Primitive Variable Computer Model) -----	29
6. Predicted Axial Pressure Distribution as a Function of Inlet Velocity (Primitive Variable Computer Model) -----	30
7. Predicted Combustor and Aft Mixing Chamber Radial Temper- ature Variations (Primitive Variable Computer Model) -----	31
8. Predicted Radial Temperature Distributions ( $\psi$ - $\omega$ Computer Model - Figure 8 of Reference 5) -----	32
9. Effect of Air Flow Rate on Predicted Flame Location and Flow Reattachment Point in the Aft Mixing Region -----	33
10. Effect of Fuel Grain Dump Inlet Geometry on Flame Zone in the Aft Mixing Region -----	34

## 1. INTRODUCTION

During the past few years, there have been many advancements in the numerical techniques for predicting the behavior of complex fluid flows. For example, several computer models have been developed by Gosman, Spalding and others [1,2,3] which use the mass, momentum and energy conservation equations reduced to finite difference, nonlinear algebraic form. The development of reliable computer programs of this type greatly benefits engineering analysis in such widely varying fields as meteorology, aerodynamics and gasdynamics.

The earlier two-dimensional computer codes were based on vorticity ( $\omega$ ) and stream function ( $\psi$ ) [1,2,4]. This form of the governing equations eliminates pressure and velocity from immediate consideration. Pressure is normally calculated only after a converged solution is obtained. This technique has several inherent disadvantages:

1. It results in large errors in the predicted pressure distributions in all but quiescent flow regions due to the higher order dependence of the pressure gradient on stream function [5].
2. It is usually restricted to constant density flows or to flows in which density varies only with temperature [3,5].
3. The boundary conditions are difficult to specify [3,5].
4. Considerable difficulty has been experienced in arriving at converged solutions, especially for nonuniformly spaced grids and high flow rates [2,4,5].
5. The  $\psi$ - $\omega$  model is not easily extended to three dimensional flows [3].

To overcome these difficulties, emphasis has been placed on developing computer codes based on velocity and pressure, the primitive variables.

A major problem with any new computer model is model validation. The difficulties of collecting accurate empirical data are multiplied when investigating three dimensional and/or reacting flows. In addition, many variables within these flows are not readily measurable (turbulence intensities, etc.).

An effort to utilize elliptic computer models which can handle turbulent, reacting, variable density flows at high subsonic and sonic velocities has been underway at the Naval Postgraduate School for several years. Two specific areas which have been investigated are flows in a turbojet test cell and in the combustion environment of a solid fuel ramjet.

A solid fuel ramjet (SFRJ) most often consists of a solid fuel grain which provides the walls for the combustion chamber [4]. Located at the air inlet end of the combustor is a sudden expansion or other type of flame stabilization device. The opposite end, downstream of the fuel grain, may also incorporate a sudden expansion aft mixing chamber. The primary combustion region contains a turbulent diffusion flame which emanates from the forward recirculation zone and remains within the developing boundary layer. The aft mixing region may incorporate some means of injecting air (bypass air) in order to complete the consumption of the fuel which exits the aft end of the fuel grain. Mixing chamber and inlet design variables, fuel grain design and fuel properties make a wide variety of performance characteristics available.

The possibility of incorporating this type of propulsion device into a future medium or long-range tactical weapon system coupled with the expense of testing each new design, makes the continued development of reliable computer models highly desirable. The model could be used to predict the effects of fuel properties and to inexpensively evaluate different geometries and operating conditions. In addition, a three dimensional code would allow modeling discrete air injection into the aft mixing region. The latter technique can substantially increase combustion efficiency and allowable fuel loading.

Previous work at the Naval Postgraduate School has been directed toward improvement of the quantitative accuracy of the  $\psi$ - $\omega$  model and toward validation of that model [4]. Reasonable agreement with empirical data has been obtained. However, as previously stated, the  $\psi$ - $\omega$  model does not predict accurate pressure distributions and numerical difficulties prevented modeling the aft mixing chamber.

The purpose of this investigation was to adapt and validate a primitive variable, two-dimensional, finite difference computer code which models the flow within a solid fuel ramjet.

## II. MODEL OVERVIEW

### A. INTRODUCTION

The computer model used in this study was adapted from the CHAMPION 2/E/FIX computer program developed by Pun and Spalding [6]. CHAMPION is a TWO-dimensional Elliptic, FIXed grid computer program which provides a solution of the conservation equations for recirculating flows in finite difference form.

### B. ASSUMPTIONS

The flow was assumed to be steady, two-dimensional and subsonic. For simplicity the value of specific heat ( $C_p$ ) was assumed to be constant although its dependence on temperature and/or composition could easily be included.

A modified Jones-Launder [6,7,8,9] two parameter turbulence model was incorporated to calculate the effective viscosity. It uses five empirical constants (Table I) and requires that two additional variables, turbulence kinetic energy ( $K$ ) and turbulence dissipation rate ( $\epsilon$ ), be evaluated. Effective viscosity was calculated using the formulas:

$$\mu_{eff} = \mu_{lam} + \mu_t \quad (1)$$

where

$$\mu_t = C_D \rho K^2 / \epsilon \quad (2)$$

$C_1$	$C_2$	$C_D$	$\sigma_{k,eff}$	$\sigma_{\epsilon,eff}$
1.43	1.92	0.09	1.0	1.3

TABLE I. K- $\epsilon$  TURBULENCE MODEL EMPIRICAL CONSTANTS

For reacting flows, the four species, oxygen, nitrogen, fuel, and products, were considered. Simple, one-step, infinitely fast kinetics were assumed in which a fuel combines with an oxidant to form a single product without intermediaries [4,10].



Fuel and oxygen, therefore, could not exist simultaneously and the combustion process was mixing limited. In addition, it was assumed that no oxygen existed at the fuel surface and that surface was isothermal. The turbulent Prandtl and Schmidt numbers were taken equal to unity and, therefore, the turbulent Lewis number was unity. The laminar Prandtl number was also taken to be unity.

### C. GOVERNING EQUATIONS

The conservation equations for axi-symmetrical flows with no tangential variations can be put into the general form [6]:

$$\underbrace{\frac{\partial}{\partial x}(\rho u \phi) + \frac{1}{r} \frac{\partial}{\partial r}(\rho r v \phi)}_{\text{convection terms}} - \underbrace{\frac{\partial}{\partial x}(\Gamma_{\phi} \frac{\partial \phi}{\partial x}) - \frac{1}{r} \frac{\partial}{\partial r}(r \Gamma_{\phi} \frac{\partial \phi}{\partial r})}_{\text{diffusion terms}} = \underbrace{S_{\phi}}_{\text{source terms}} \quad (3)$$

where  $\phi$  stands for the dependent variable ( $u, v, k, \epsilon, h$ , etc..) being considered ( $\phi = 1$  for the continuity equation),  $\Gamma_{\phi}$  is the appropriate effective exchange coefficient for turbulent flow and  $S_{\phi}$  is the "source term" (Table II). The energy equation in terms of stagnation enthalpy has no source terms since the turbulent Prandtl and Schmidt numbers were chosen as unity and radiative transport was neglected [1,3]. Thus the



$\phi$	$\Gamma_\phi$	$S_\phi$
u	$\mu_{\text{eff}}$	$-\frac{\partial P}{\partial x} - \frac{2}{3} \frac{\partial}{\partial x} \left\{ \frac{\mu}{r} \left[ \frac{\partial}{\partial x} (ru) + \frac{\partial}{\partial r} (rv) \right] \right\} + \frac{\partial}{\partial x} \left( \mu \frac{\partial u}{\partial x} \right) + \frac{1}{r} \frac{\partial}{\partial r} \left( \mu r \frac{\partial v}{\partial x} \right)$
v	$\mu_{\text{eff}}$	$-\frac{\partial P}{\partial r} - 2 \frac{\mu v}{r^2} - \frac{2}{3} \frac{\partial}{\partial r} \left\{ \frac{\mu}{r} \left[ \frac{\partial}{\partial x} (ru) + \frac{\partial}{\partial r} (rv) \right] \right\} + \frac{\partial}{\partial x} \left( \mu \frac{\partial u}{\partial r} \right) + \frac{1}{r} \frac{\partial}{\partial r} \left( \mu r \frac{\partial v}{\partial r} \right)$
TKE	$\mu_{\text{eff}}/\sigma_k$	$\mu_t \left( 2 \left[ \left( \frac{\partial u}{\partial x} \right)^2 + \left( \frac{\partial v}{\partial r} \right)^2 + \left( \frac{v}{r} \right)^2 \right] + \left( \frac{\partial u}{\partial r} + \frac{\partial v}{\partial x} \right)^2 \right) - \rho \epsilon$
TED	$\mu_{\text{eff}}/\sigma_\epsilon$	$\frac{C_{1\epsilon}}{k} \left( \mu_t \left( 2 \left[ \left( \frac{\partial u}{\partial x} \right)^2 + \left( \frac{\partial v}{\partial r} \right)^2 + \left( \frac{v}{r} \right)^2 \right] + \left( \frac{\partial u}{\partial r} + \frac{\partial v}{\partial x} \right)^2 \right) \right) - \frac{C_{2\epsilon} \rho \epsilon}{k}$
h	$\mu_{\text{eff}}/\sigma_h$	0
$m_{fu} - \frac{m_{ox}}{l}$	$\mu_{\text{eff}}/\sigma_j$	0
$m_{N2}$	$\mu_{\text{eff}}/\sigma_j$	0

$$\sigma_j = \sigma_k = \sigma_h = 1, \quad \sigma_\epsilon = 1.3$$

TABLE II. GOVERNING EQUATION PARAMETERS

stagnation enthalpy is given by:

$$\tilde{h} = h + (u^2 + v^2)/2 + K \quad (4)$$

where for non-reacting flows:

$$h \equiv c_p T \quad (5)$$

and for reacting flows:

$$h \equiv m_{ox} \Delta H/i + c_p (T - T_{ref}) \quad (6)$$

The calculation of temperature was made using equations (4), (5) and (6). Density was calculated from the perfect gas law:

$$\rho = P/RT \quad (7)$$

for non-reacting flows:  $R = \text{constant}$

$$\text{for reacting flows: } R = \bar{R}/\bar{M} \quad (8)$$

where,

$$1/\bar{M} = m_{fu}/M_{fu} + m_{ox}/M_{ox} + m_{N2}/M_{N2} + m_{pr}/M_{pr} \quad (9)$$

For modeling reacting flows, two additional quantities,  $m_{N2}$  and  $\chi \equiv m_{fu} - m_{ox}/i$ , were evaluated. Each of these properties as well as stagnation enthalpy have identical governing differential equations (equation (3) with no source terms). In appropriate dimensionless form they also have identical boundary conditions. Thus, only one of the equations had to be solved. The dimensionless form selected for each property was:

$$H = (\tilde{h}_{in} - \tilde{h})/(\tilde{h}_{in} - \tilde{h}_{fg}) \quad (10)$$

$$\bar{m}_{N2} = (m_{N2_{in}} - m_{N2}) / (m_{N2_{in}} - m_{N2_{fg}}) \quad (11)$$

$$\bar{\chi} = (\chi - \chi_{in}) / (\chi_{fg} - \chi_{in}) \quad (12)$$

In this study, stagnation enthalpy was calculated.  $H$  was then formed using equation (10). Since  $H = \bar{m}_{N2} = \bar{\chi}$  at all points in the flow field,  $m_{N2}$  and  $\chi$  could be calculated using equations (11) and (12). The mass fractions of fuel, oxygen, and products ( $m_{fu}$ ,  $m_{ox}$ ,  $m_{pr}$ ) were found from the equations:

$$\text{for } \chi \geq 0; \quad m_{fu} = \chi, \quad m_{ox} = 0 \quad (13)$$

$$\text{for } \chi < 0; \quad m_{fu} = 0, \quad m_{ox} = -\chi$$

$$m_{pr} = 1 - m_{pr} - m_{ox} - m_{fu} - m_{N2} \quad (14)$$

#### D. CONSERVATION OF MASS

On each radial line the mass flow rate was calculated using the local density. The error in mass flow (compared to the summation of "mass-in" at all upstream boundaries) was used to uniformly adjust the axial velocity over the entire line. This process ensured that overall continuity was satisfied on the line. The pressure at all downstream locations was then adjusted to approximately correct for the momentum imbalance created by the uniform axial velocity adjustment. A "pressure correction" equation was then solved for each cell on the line. Local cell velocity (axial and radial) and pressure were then adjusted to satisfy cell-wise continuity. The details of this procedure are presented in reference 6.

## E. BOUNDARY CONDITIONS

### 1. Introduction

Fixed boundary conditions were specified at the desired or experimentally determined values. Specified gradient boundary conditions were handled by setting the appropriate convection/diffusion coefficient to zero in the finite difference equation ("breaking the link") and then entering the appropriate gradient through linearized "false" source terms [6]. The geometry and appropriate boundary conditions are summarized in figure 1.

### 2. Inlet

Although not a computer program limitation, "plug flow" was assumed at the inlet. Turbulence kinetic energy was selected to be uniform with a value which corresponded to the approximate turbulence intensity of the inlet flow.

### 3. Axis of Symmetry and Exit Plane

Radial and axial gradients were set equal to zero on the center line and exit respectively. The radial flow velocity was equated to zero.

### 4. Solid Boundaries

All non-reacting solid boundaries were considered adiabatic with both velocity components equal to zero ("no slip" condition).

For simplicity, a two part boundary layer was used. The border between the laminar sublayer and the turbulent layer was taken at

$y_p^+ = 11.5$  [6].  $y_p^+$  was evaluated at each near wall node (p),

$$y_p^+ = (\rho \delta / \mu_{lam}) (\tau_w / \rho)^{1/2} \quad (15)$$

where, for  $y_p^+ \geq 11.5$

$$\tau_w = c_D^{1/2} \rho K_p \quad (16)$$

$\tau_w$  was assumed uniform from the wall to the near wall grid point. Thus,

$$y_p^+ = c_D^{1/4} \rho K_p^{1/2} \delta / \mu_{lam} \quad (17)$$

If  $y_p^+ \geq 11.5$ , the wall shear stress ( $\tau_w$ ) was calculated using the formula:

$$\begin{aligned} \tau_w &= c_D^{1/2} \rho K_p = \rho c_D^{1/4} K_p^{1/2} (u/u^+) \\ &= \kappa c_D^{1/4} \rho u_p K_p^{1/2} / \ln(E \rho \delta c_D^{1/4} K_p^{1/2} / \mu_{lam}) \end{aligned} \quad (18)$$

where

$$u^+ \equiv \frac{1}{\kappa} \ln(E y_p^+) \quad (19)$$

Wall shear stress was evaluated for  $y_p^+ < 11.5$  from the formula:

$$\tau_w = \mu_{lam} u_p / \delta \quad (20)$$

Due to the steep gradients of properties in turbulent flows near solid boundaries, the source terms for  $K$  and  $\epsilon$  at near wall nodes were expressed in terms of the wall shear stress [1,6].  $\tau_w$  also provides the boundary condition for the  $u$  and  $v$  equations. In the following equation for turbulence dissipation rate ( $\epsilon$ ) at a near wall node ( $p$ ), the length scale is presumed proportional to the distance from the wall ( $\delta$ ).

$$\epsilon_p = c_D^{3/4} K_p^{3/2} / \kappa \delta = K_p^{3/2} / 2.43 \delta \quad (21)$$

It was found, as was previously found by Netzer [4], that (when using the sudden expansion geometry in reacting flows) the near wall dissipation had to be increased on the step face ( $\epsilon_p = K_p^{3/2}/0.4\delta$ ) and that the grid spacing adjacent to the fuel surface had to be fine ( $y_p^+ < 11.5$ ) in order to obtain a temperature distribution in qualitative agreement with experiment. Equation (20) implies that the wall shear stress is calculated assuming a linear velocity profile when  $y_p^+ < 11.5$ . A near-wall grid point, therefore, can lie within the laminar sublayer, but the source terms for  $K$  and  $\epsilon$  imply that  $\mu_{eff}/\mu_{lam}$  is much greater than one [7,8]. This fact precludes  $y_p^+$  from being significantly less than 11.5.

For reacting flows, the boundary conditions for the dimensionless properties (equations (10), (11) and (12)) were zero at the inlet and unity "deep" in the fuel grain (fg). These properties were considered to have zero gradients on non-reacting surfaces.

The assumptions employed for reacting flows (unity turbulent Prandtl and Schmidt numbers, simple chemical reaction, constant specific heat and stagnation enthalpy defined in equations (4) and (6)) result in a general boundary condition for all "conserved" properties ( $\phi_c$ ) [10] on a surface which has mass transfer,

$$\dot{m}'_{bw} = (\Gamma_\phi \frac{\partial \phi_c}{\partial r})_{bw} / (\phi_{c_{bw}} - \phi_{c_{fg}}) \quad (22)$$

where  $\phi_c$  represents  $\tilde{h}$ ,  $m_{N2}$  or  $\chi \equiv m_{fu} - m_{ox}/I$ .

A mass transfer conductance ( $g$ ) is often defined such that,

$$(\Gamma_\phi \frac{\partial \phi_c}{\partial r})_{bw} = g(\phi_{c_\infty} - \phi_{c_{bw}}) \quad (23)$$

where  $\phi_{c_\infty}$  is defined as the free stream value. For this application,  $\phi_{c_\infty}$  was taken to be the local near wall value  $\phi_{c_p}$ .

Substituting equation (23) into equation (22) yields:

$$\dot{m}''_{bw} = g(\phi_{c_p} - \phi_{c_{bw}})/(\phi_{c_{bw}} - \phi_{c_{fg}}) \quad (24)$$

$$\equiv g \text{ BP} \quad (25)$$

where BP represents the mass transfer (or "blowing") parameter.

Without mass transfer the wall heat flux ( $\dot{q}_w''$ ) can be defined in terms of the conditions at the near wall node.

$$\dot{q}_w'' = \frac{h}{C_p}(h_w - h_p) = - \left( \frac{\tilde{K}}{C_p} \frac{\partial h}{\partial r} \right)_w \quad (26)$$

where  $h_w$  is the enthalpy of the wall and  $h$  is the heat transfer conductance.

With  $\phi_c = h$  in equation (23),

$$g = \left( \frac{\tilde{K}}{C_p} \frac{\partial h}{\partial r} \right)_w / (h_p - h_w) \quad (27)$$

Substituting equation (26) into equation (27) yields:

$$g = h/C_p \quad (28)$$

or

$$g/(\rho u)_p = h/[(\rho u)_p C_p] \equiv St \quad (29)$$

thus,

$$g = (\rho u)_p St \quad (30)$$

From Reynolds Analogy with unity Prandtl number,

$$St = C_f/2 = \tau_w/(\rho u^2)_p \quad (31)$$

where  $C_f$  is the local friction coefficient.

Combining equations (30) and (31) yields:

$$g = \tau_w / u_p \quad (32)$$

Using the Couette flow approximation for the boundary layer behavior with mass transfer [10],

$$g = g^* \ln(1 + BP) / BP \quad (33)$$

where

$$g^* \equiv \lim_{BP \rightarrow 0} (g) \quad (34)$$

In this application, BP was evaluated from the solution of the energy equation using,

$$BP = (\tilde{h}_p - \tilde{h}_{bw}) / (\tilde{h}_{bw} - \tilde{h}_{fg}) \quad (35)$$

The wall shear stress was calculated using equation (18) or equation (20) and modified with equation (33).

$$\tau_{bw} = \tau_w \ln(1 + BP) / BP \quad (36)$$

where  $\tau_w$  is the wall shear stress without wall mass addition.

The mass transfer conductance (g) was found using equation (32). The wall mass flux was then evaluated using equation (25).

The wall heat flux ( $\dot{q}_w''$ ) on all solid isothermal boundaries was evaluated using the Reynolds analogy:

$$-\dot{q}_w'' / (\tilde{h}_p - \tilde{h}_w) = \tau_w / u_p \quad (37)$$



Since the blowing rates were small for the solid fuel ramjet (typically,  $BP < 2.0$ ),  $K$  and  $\epsilon$  were evaluated using equation (3) and the terms presented in Table II which incorporate the empirical constants of Table I.

Blowing velocity ( $v_{bw}$ ) and fuel regression rate (RR) were calculated using the formulas:

$$v_{bw} = -\dot{m}_{bw}''/\rho_{bw} \quad (38)$$

$$RR = \dot{m}_{bw}''/\rho_{fg} \quad (39)$$

#### F. SOLUTION PROCEDURE

Five variables ( $u, v, K, \epsilon$  and  $H$  or  $h$ ) were solved using equation (3) in finite difference form. The line by line iterative procedure employed upwind differencing and under relaxation to promote convergence [6]. Pressure (relative to a selectable position and magnitude within the grid) was obtained from the mass conservation imposed on each radial grid line and on each nodal control volume as discussed above. Effective viscosity, temperature and density were also obtained as described above. A more detailed explanation of this procedure can be found in reference 6.

### III. DISCUSSION OF RESULTS

#### A. INTRODUCTION

The purpose of this study was to develop a primitive variable, finite-difference computer program that could be used to determine the flow within a solid fuel ramjet combustor with emphasis on the aft mixing chamber. The effects of inlet mass flow rate and inlet dump area ratio on the flow field were examined. As previously explained, an aft mixing region allows further combustion aft of the fuel grain. This process normally increases combustion efficiency. Lowering the inlet flow rate increases the fuel-air ratio within the fuel port. Bypass air can then be injected into the aft mixing region. The latter procedure can be used to appreciably increase fuel loading. Previous work at the Naval Postgraduate School [4,11,12] modeled a SFRJ with a computer program utilizing  $\psi$ - $\omega$  as primary variables. Numerical instabilities, however, prevented the use of the  $\psi$ - $\omega$  model to predict the flow in the aft mixing region. The results of that investigation and some empirical data were available for comparison with the predictions from the primitive variable model.

Several factors were anticipated which could contribute to differences between the predictions of the two models and the empirical data:

- a. Some of the experimental data were measured in cold, nonreacting flows.
- b. The incorporation of the aft mixing chamber into the primitive variable model could influence the flow upstream in the combustion chamber.
- c. In the  $\psi$ - $\omega$  model, a wall value of turbulence kinetic energy ( $K$ ) was specified through a slip factor such that  $K_w = (-1.0 \text{ or } -0.39) * K_p$ ,

depending on the magnitude of the turbulent Reynolds Number. In the u-v-p model the boundary condition for K at the near wall node (p) was specified in terms of the wall shear stress. In addition, in the primitive variable model, the boundary condition for stagnation enthalpy at the near wall node was made a function of wall shear stress through the Reynolds Analogy. These factors affect heat flux to the wall, and, therefore, the fuel regression rate.

d. The u-v-p model incorporated a 23 by 21 grid in the fuel port while the  $\psi$ - $\omega$  model utilized a 17 by 25 grid. In reality the heat of vaporization of the fuel is a fixed quantity and, if converged solutions are obtained, the wall heat flux should not depend upon the grid spacing. However, it has been found [4] that the heat flux to the wall (which is calculated using the near-wall grid point) is a function of the grid distance from the wall. This results from the assumed behavior of the variables near the wall. The procedure employed in this study was to adjust the heat of vaporization to match the empirical fuel regression rate at one air flow rate and to use that value for all other flow rates. If the model is realistic, fuel regression rate should then vary with air flow rate in agreement with experiment.

#### B. REGRESSION RATE

Figure 2 shows that the fuel regression rate predictions of the u-v-p and  $\psi$ - $\omega$  models are quite similar. Both predict the peak regression rate upstream of experiment and have similar slopes. This early peak in the regression rate results from the model predicting a shorter reattachment length than was found experimentally [4]. The primitive variable model

predicted higher regression rates downstream of flow reattachment in better agreement with experiment.

Figure 3 shows the effects of increasing inlet air mass flux ( $G = \dot{m}_{air}/A_{fp} \propto V_{in}$ ) on fuel regression rate ( $\dot{r}_{fu}$ ). The regression profile remained the same and, as expected, decreased with decreasing  $G$ . It has been found experimentally that the regression rate of plexiglass varies as the air mass flux raised to a constant power ( $\dot{r}_{fu} \propto G^n$ ). Boaz and Netzer [11] found that this constant was equal to 0.41 while Mady, et al [12] found it to be approximately 0.38. For the three test cases of this study, the u-v-p model predicted the constant,  $n$ , to be between 0.31 and 0.34. Thus, the primitive variable model appears to correctly predict the nature of the change in convective heat flux to the fuel surface with air flow rate.

#### C. TURBULENCE INTENSITY

Figure 4 compares the predicted centerline turbulence intensity (assuming isotropic turbulence) and experimental data for non-reacting flow. The primitive variable computer model slightly underpredicted the peak turbulence intensity while the  $\psi$ - $\omega$  model overpredicted it. Both models predicted the peak occurring downstream of experiment and both distributions appear to approach an identical asymptote downstream. The decrease in turbulence intensity predicted by the  $\psi$ - $\omega$  model near the inlet resulted from the model over-predicting the velocity increase as the air entered the combustor [4]. The u-v-p model overcame this difficulty. The differences in the results from the two computer models may result from the differences in the boundary conditions on turbulence

kinetic energy in the combustor and/or to the effects of the addition of the aft mixing chamber on the upstream flow. It should also be noted that the experimental data used in this comparison were obtained in a non-reacting flow.

Figure 5 shows the effect of decreasing inlet air mass flux on turbulence intensity. As anticipated, the peak turbulence intensity decreased as inlet axial velocity decreased. Each test condition, however, converged on the same value downstream. Much additional experimental work is required to obtain the turbulence intensities in reacting flows; only then can the adequacy of the K- $\epsilon$  turbulence model be fully evaluated.

#### D. PRESSURE

Figure 6 shows the effect of inlet velocity on the axial pressure distributions for the three primitive variable test conditions (Table III). (The radial scale has been expanded to illustrate the pressure variations. The maximum pressure variation is approximately 1.2 psi.) The radial location of these distributions is given as a fraction of the fuel port radius ( $R_{fp}$ ). As expected, pressure initially increased due to jet spreading. This was followed by a slight pressure drop as the flow accelerated due to heat addition and wall friction. The final pressure rise was due to jet spreading in the aft mixing region.

#### E. TEMPERATURE

Figure 7 displays radial temperature variations in the combustor near the end of the full grain and at about 1.5 aft mixing region diameters down the aft chamber. As discussed above, fuel flow rate decreases less than inlet air flow rate ( $\dot{P}_{fu} \propto G^n$ ,  $n < 1$ ). Therefore,

CASE	$r_{In}$ (m)	$\dot{m}_{air}$ (kg/sec)	$u_{In}$ (m/sec)	$\dot{G}$ (kg/m <sup>2</sup> -sec)
1	.00681	.08049	197.0	70.6
2	.00681	.07274	178.0	63.8
3	.00681	.06442	157.6	56.5

TABLE III. SOLID FUEL RAMJET TEST CONDITIONS

as air flow rate is decreased, the overall mixture ratio becomes more fuel rich, and the developing boundary layer and the fuel layer between the diffusion flame and the wall thicken. Thus, as shown in figure 7, as the inlet velocity (and, therefore, the inlet air mass flux) was decreased, the maximum temperature (or "flame") in the combustor moved away from the fuel grain and the centerline temperature increased. The maximum temperature in the aft mixing chamber was also predicted to occur farther from the top wall.

Figure 8 shows similar data predicted by the  $\psi$ - $\omega$  model slightly farther upstream. A significant difference between the predictions of the two computer models was that the  $\psi$ - $\omega$  model predicted a stronger dependence of the peak temperature radial location on the inlet air velocity. An aft mixing region was not incorporated into the  $\psi$ - $\omega$  model. Therefore, the boundary layer continued to grow and the point of maximum temperature continued to recede from the fuel surface with increasing axial distance from the initial reattachment point. The aft mixing region of the u-v-p model caused the boundary layer thickness (and, therefore, the location of the peak temperature) to become approximately constant in the latter portion of the combustion chamber. This was the apparent cause of the weaker dependence predicted by the u-v-p model of peak temperature location and boundary layer thickness on inlet air mass flux.

Figure 9 is an illustration of the predicted combustion behavior in the aft mixing region. (The radial dimension has been expanded for clarity.) Lines of maximum temperature (i.e., the flame sheet location) are presented as a function of fuel grain inlet air velocity. It should be noted

that the aft recirculation zone, which is also depicted on this figure, was predicted to be fuel rich and did not vary appreciably in size with changing inlet air mass flux. As discussed above, the fuel regression rate decreased more slowly than inlet air flow rate. Thus, as air flux was decreased the mixture entering the aft chamber became more fuel rich and the thickness of the fuel layer at the end of the fuel grain increased slightly. With high air mass flux through the fuel port the mixture ratio is fuel lean. The flame therefore propagates to the outer wall of the aft mixing chamber. This condition could be expected to produce a high combustion efficiency. It should be noted that an adequate length-to-diameter ratio is required to allow the flame to spread to the wall. This ratio is apparently a function of the fuel port to aft mixing chamber cross-sectional area ratio. As the air flow rate was decreased the mixture ratio became fuel rich and the flame did not reach the wall. This would result in unburned fuel entering the nozzle and a lower combustion efficiency. Figure 10 shows the predicted effect of the fuel inlet dump step size on the flame behavior in the aft mixing chamber. The recirculation zone did not change in size since the air mass fluxes were identical. The smaller inlet step produced a slightly higher fuel regression rate and therefore required a longer aft mixing region. These predictions might be used as a first approximation for predicting the "best" placement of bypass air dumps in the aft mixing region. To predict an optimum location, however, the primitive variable model would have to be expanded to three dimensions.



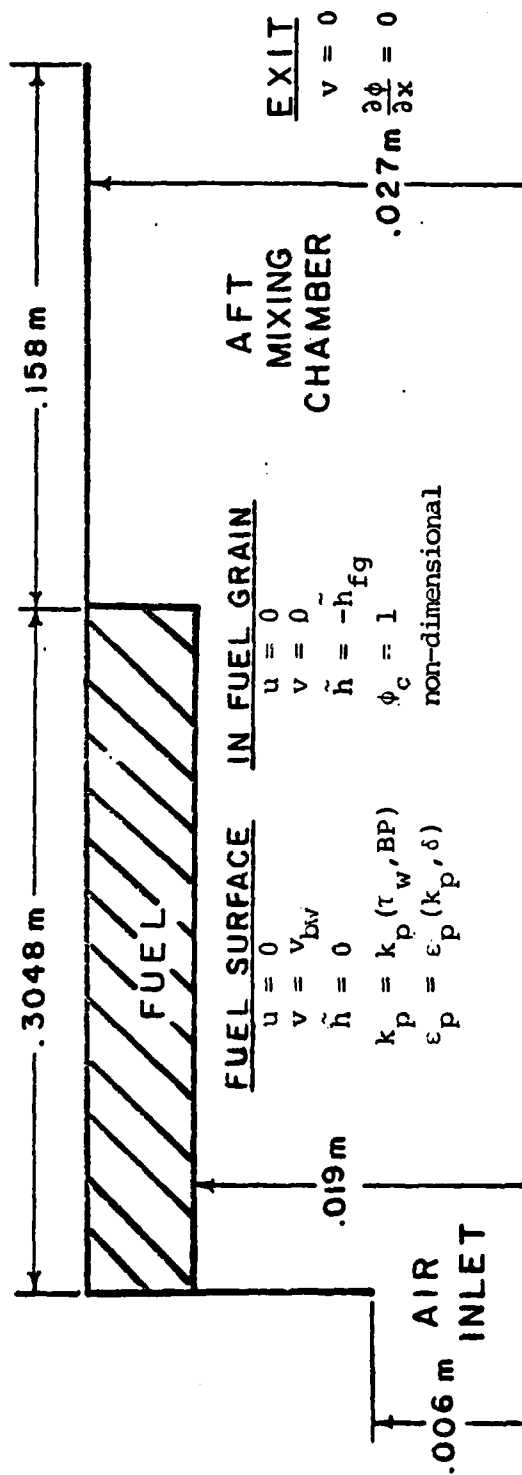
#### F. COMPUTER RELATED PROBLEMS

As has been discussed previously, in order to obtain results that were in agreement with experiment, the grid spacing near the fuel surface was required to be fine and the length scale of turbulence was decreased on the combustor step face. Because convergence was sensitive to the length-to-width ratio of individual control volumes, the small radial grid spacing near the fuel surface forced similar fine spacing in the axial direction downstream in the aft mixing region. A length to width ratio of less than ten to one was required. These criteria forced the use of a large number of cells, which in turn required a large amount of CPU time. A typical primitive variable 40 by 33 grid required 75 to 80 minutes of CPU time on an IBM 360-67 computer to converge. A typical  $\psi$ - $\omega$  model with a 17 by 25 grid required 35 to 40 minutes of CPU time. It must be remembered, however, that numerical instabilities prohibited the modeling of an aft mixing chamber with the  $\psi$ - $\omega$  model.

The primitive variable model demonstrated some convergence difficulty in the aft recirculation region. This problem seemed to be associated with the continually changing velocity profile just prior to the aft expansion (the "inlet" conditions for the aft mixing chamber). This effect was suppressed by sweeping through the entire flow field several times with only a few traverses on each line and then increasing the number of traverses on the radial grid lines in the aft mixing region once the combustor flow field had essentially converged.

#### IV. CONCLUSIONS

In general, the predicted flow fields for the two computer models were quite similar within the fuel grain. However, the presence of the aft mixing region coupled with the few boundary condition differences previously mentioned, had some effect on the flow field predictions. The most noticeable of these was the decrease in dependence of the boundary layer thickness and the maximum temperature radial location on axial inlet velocity. As anticipated, the primitive variable model allowed the prediction of the flow field within the aft mixing region. This was not possible with the  $\psi$ - $\omega$  model. Many additional empirical data are needed to completely assess the validity of the primitive variable model in predicting the flow in a SFRJ.



# INLET

$$u = u_{in}$$

$$v = 0$$

$$k = .005 \cdot u_{in}^2$$

$$\epsilon = .09k^{3/2} / .03r$$

$$X = -m_{ox,in} / i$$

$$\phi_c = 0$$

non-dimensional

# CENTER LINE

$$v = 0$$

$$\frac{\partial \phi}{\partial r} = 0$$

# NON REACTING WALLS

$$u = 0$$

$$v = 0$$

$$\frac{\partial \phi_c}{\partial x} \text{ or } \frac{\partial \phi_c}{\partial r} = 0$$

$$k_p = k_p(\tau_w)$$

$$\epsilon_p = \epsilon_p(k_p, \delta)$$

FIGURE 1. SOLID FUEL RAMJET GEOMETRY AND BOUNDARY CONDITIONS

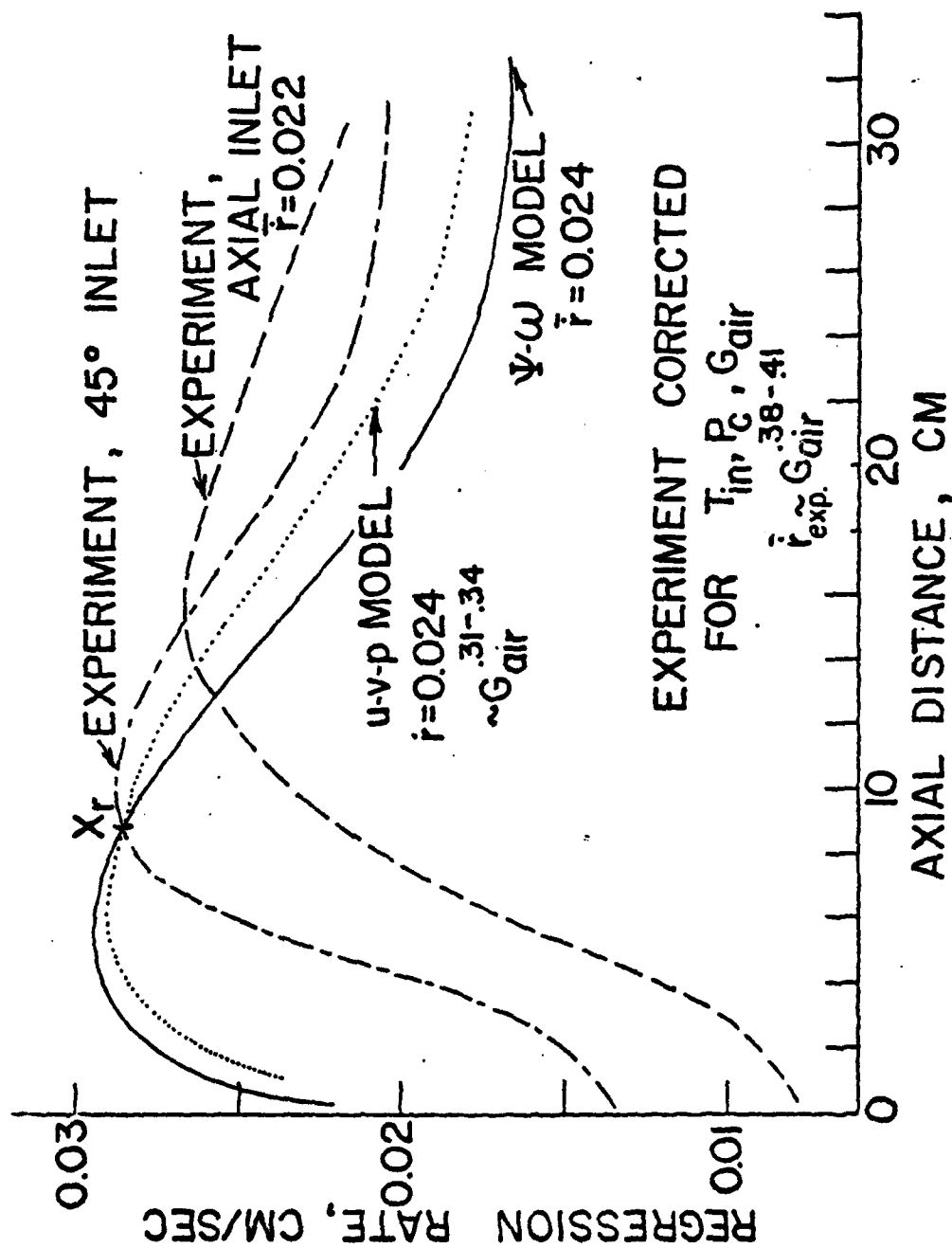


Figure 2. Plexiglass Regression Rates

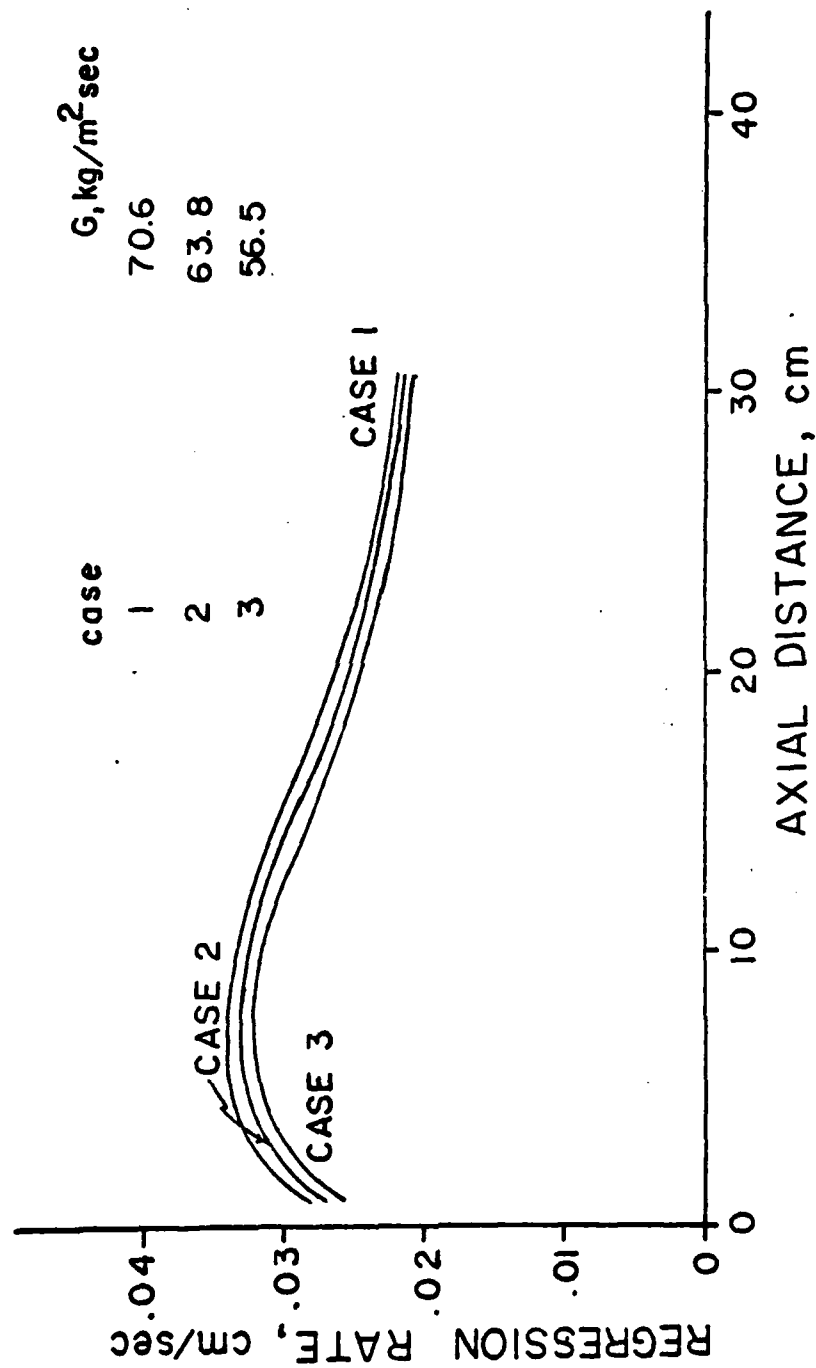


FIGURE 3. EFFECTS OF AIR MASS FLUX ON THE PREDICTED REGRESSION RATES OF THE PRIMITIVE VARIABLE COMPUTER MODEL

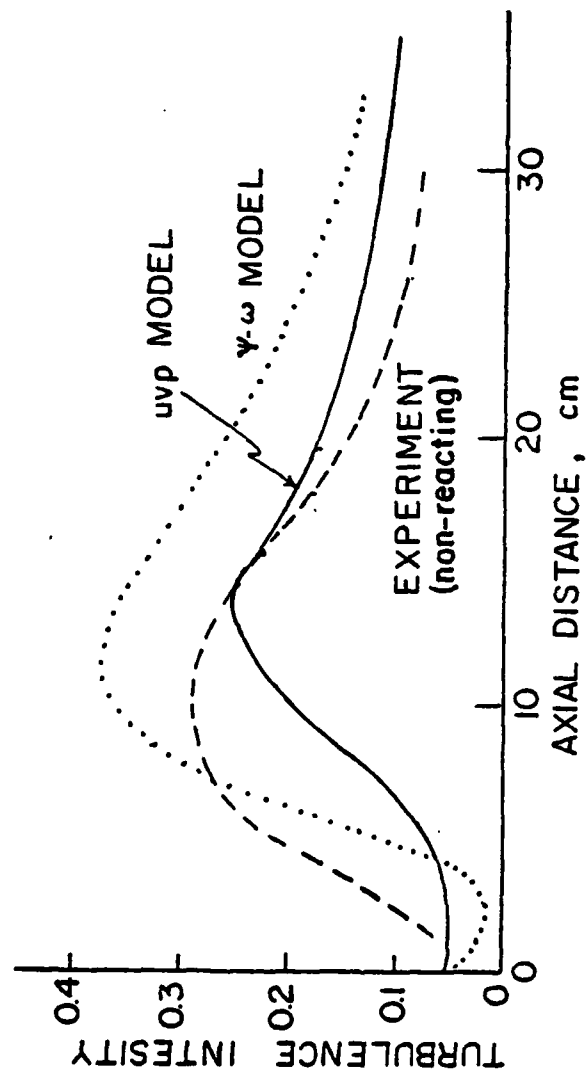


FIGURE 4. CENTERLINE TURBULENCE INTENSITY

$$(I \equiv (\frac{2}{3} k)^{1/2} / u)$$

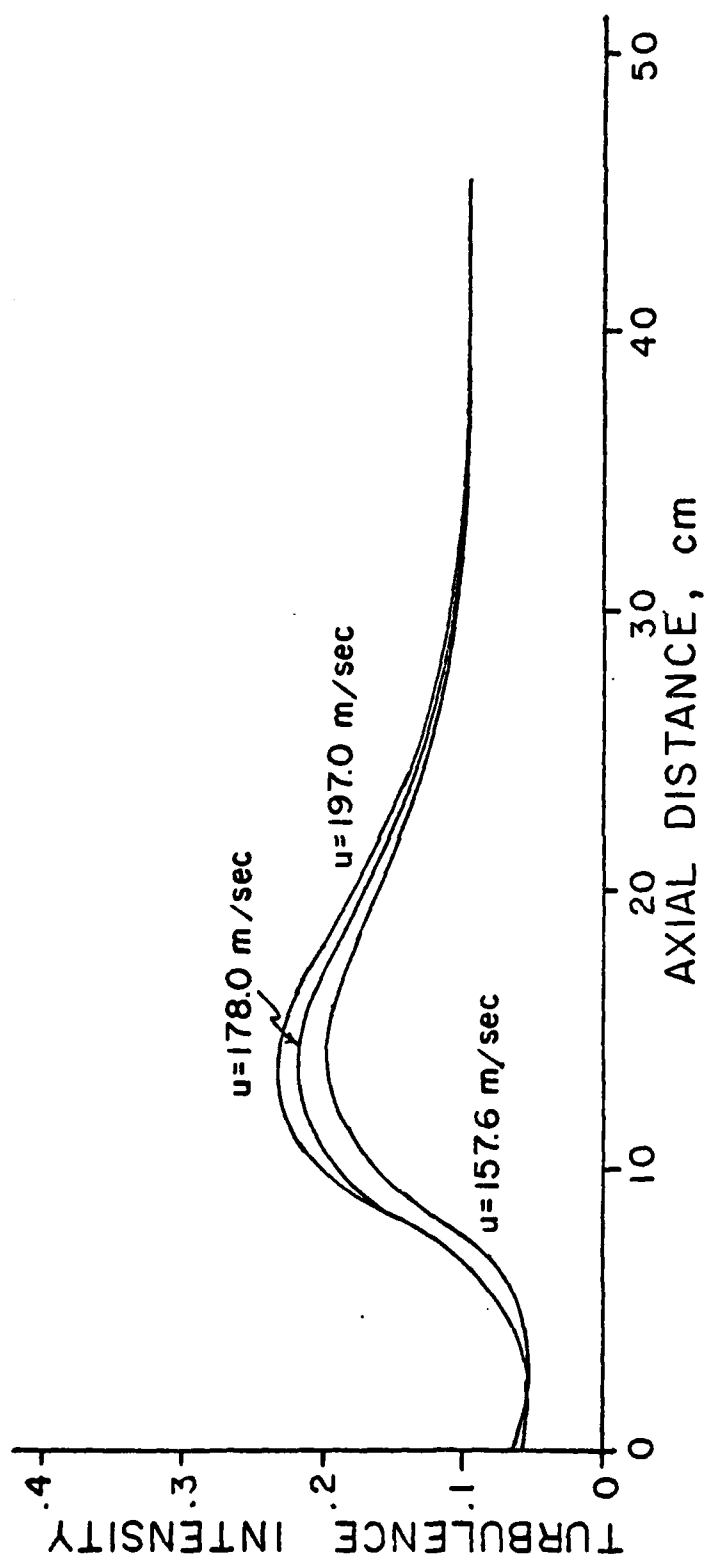


FIGURE 5. PREDICTED CENTERLINE TURBULENCE INTENSITY AS A FUNCTION OF INLET VELOCITY (PRIMITIVE VARIABLE COMPUTER MODEL,

$$I \equiv \left( \frac{2}{3} k \right)^{1/2} / u$$

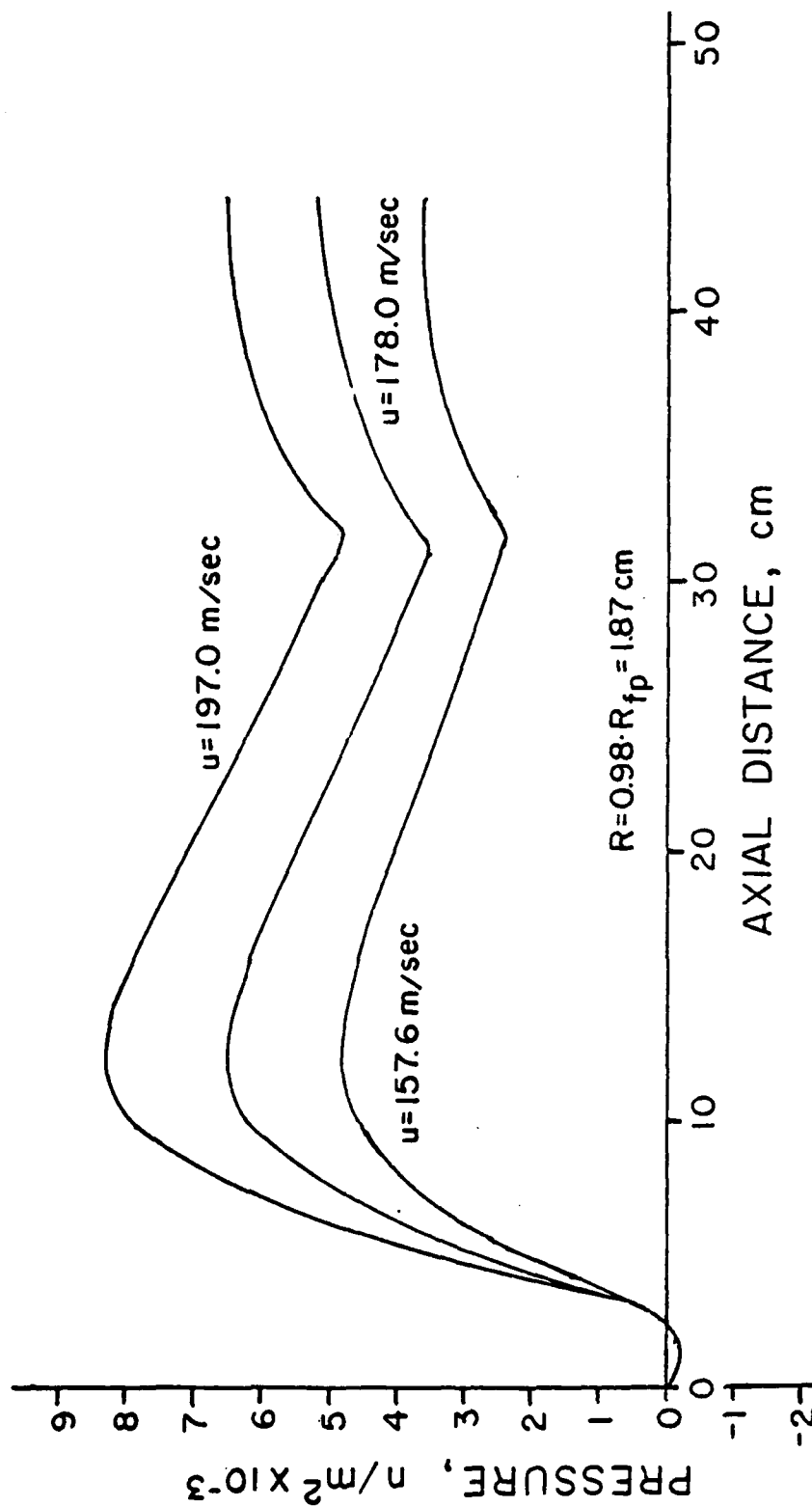


FIGURE 6. PREDICTED AXIAL PRESSURE DISTRIBUTION AS A FUNCTION OF INLET VELOCITY (PRIMITIVE VARIABLE COMPUTER MODEL)



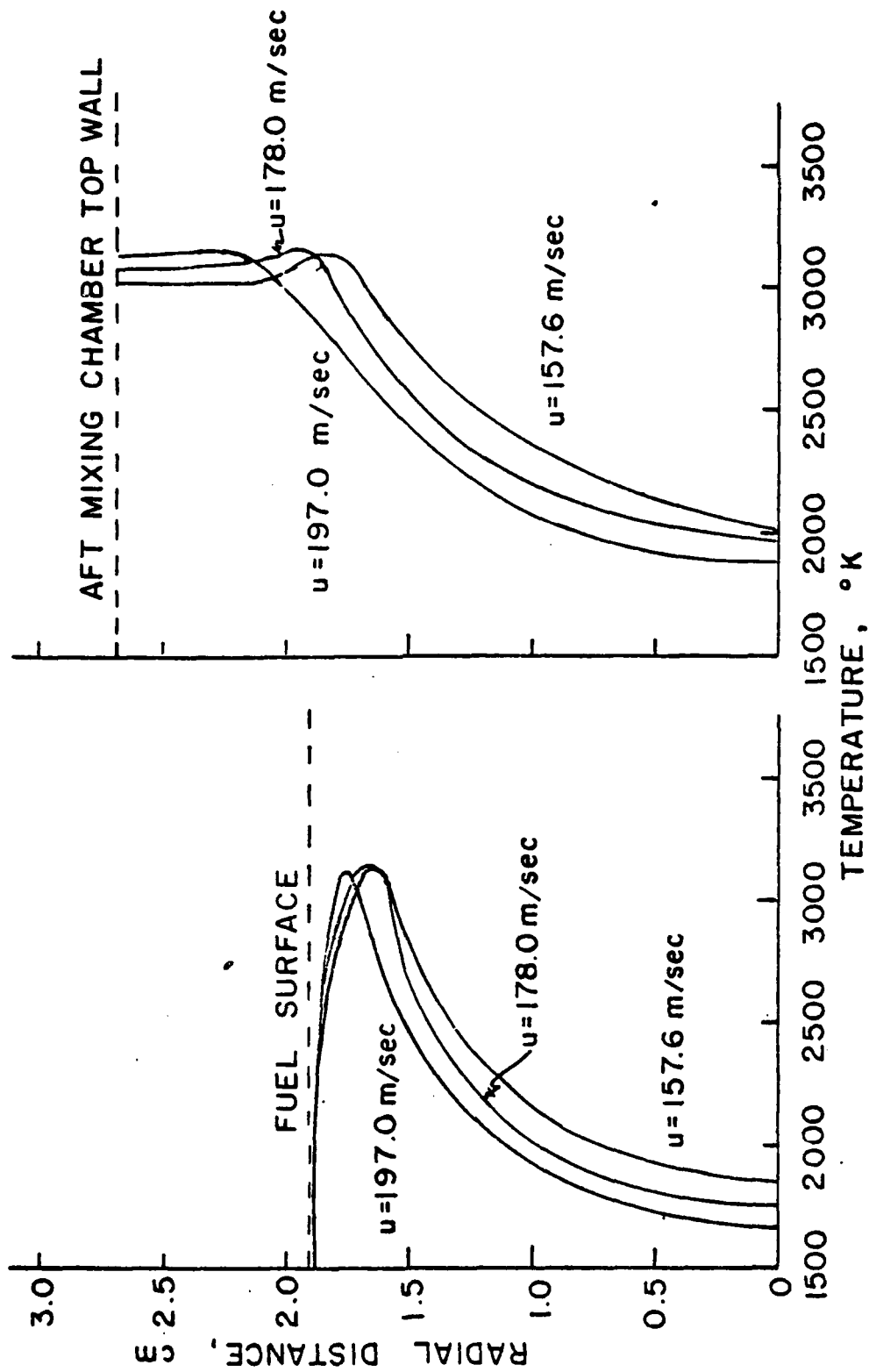


FIGURE 7. PREDICTED COMBUSTOR AND AFT MIXING CHAMBER RADIAL TEMPERATURE VARIATIONS (PRIMITIVE VARIABLE COMPUTER MODEL)

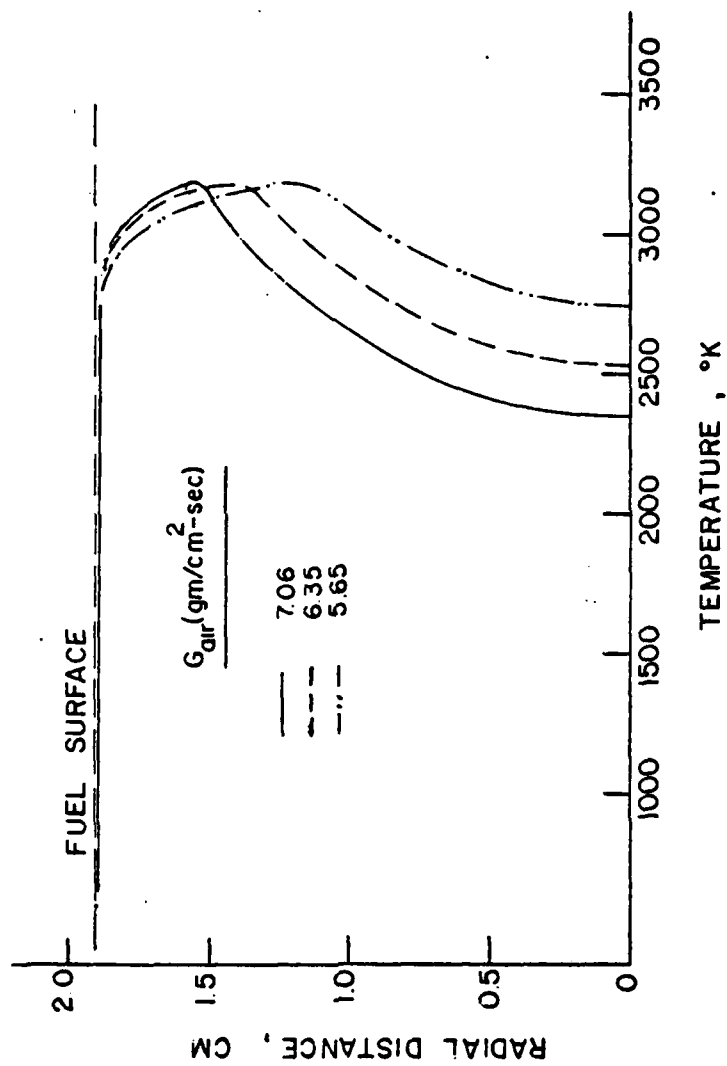


FIGURE 8. PREDICTED RADIAL TEMPERATURE DISTRIBUTIONS  
( $\psi$ - $\omega$  COMPUTER MODEL, FIGURE 8 OF REFERENCE 4)

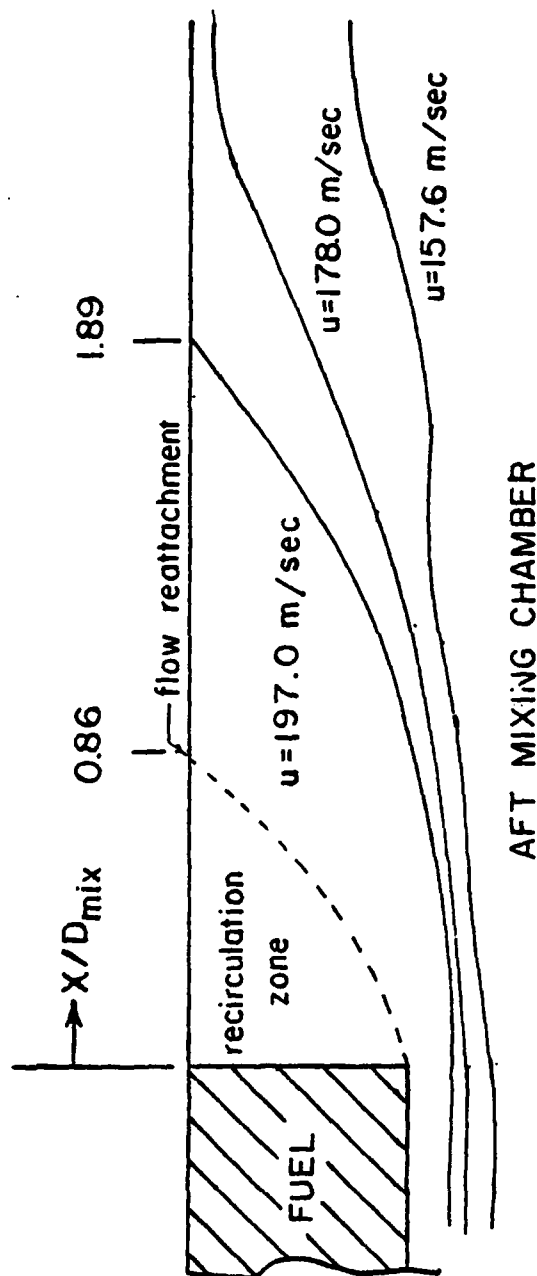


FIGURE 9. Effect of Air Flow Rate on Predicted Flame Location and Flow Reattachment Point in the Aft Mixing Region .

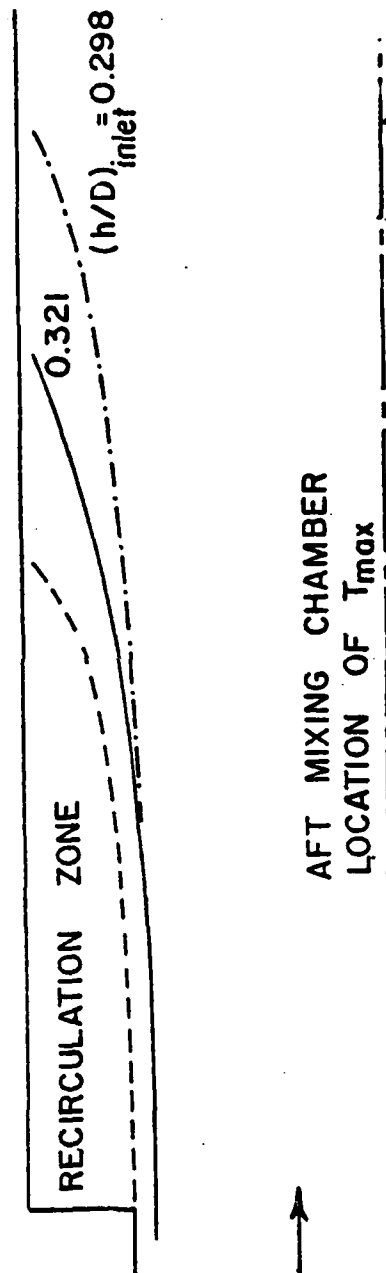


Figure 10. Effect of Fuel Grain Dump Inlet Geometry on Flame Zone in the Aft Mixing Region

## V. REFERENCES

1. Gosman, A.D., and others, Heat and Mass Transfer in Recirculating Flows, Academic Press, 1969.
2. Hayes, J.D. and Netzer, D.W., An Investigation of the Flow in Turbojet Test Cells and Augmenters, Naval Postgraduate School Report Number NPS-57Nt-75101, October 1975.
3. Mongia, H.C. and Reynolds, R.S., Combustor Design Criteria Validation Volume III, AIRESEARCH Manufacturing Company of Arizona Report Number USARTL-TR-78-55c, February 1979.
4. Netzer, D.W., "Modeling Solid-Fuel Ramjet Combustion," Journal of Spacecraft and Rockets, Volume 14, Number 12, p. 762-766, December 1977.
5. Walters, J.J. and Netzer, D.W., A Validation of Mathematical Models of Turbojet Test Cells, Naval Postgraduate School Report Number NPS67-78-002, June 1978.
6. Pun, W.M. and Spalding, D.B., A General Computer Program for Two-Dimensional Elliptic Flows, Imperial College of Science and Technology, Report No. HTS/76/2, August 1977.
7. Launder, B.E. and Spalding, D.B., "The Numerical Computation of Turbulent Flows," Computer Methods in Applied Mechanics and Engineering, p. 269-289, August 1973.
8. Jones, W.P. and Launder, B.E., "The Predictions of Laminarization with a Two-Equation Model of Turbulence," INT. J. Heat Mass, Transfer, Volume 15, p. 68-87, 1972.
9. Launder, B.E. and Spalding, D.B., Lectures in Mathematical Models of Turbulence, 2nd ed., Academic Press, 1976.
10. Kays, W.M., Convective Heat and Mass Transfer, McGraw-Hill, 1966.
11. Boaz, L.D. and Netzer, D.W., An Investigation of the Internal Ballistics of Solid Fuel Ramjets, Naval Postgraduate School Report Number NPS-57Nt-73031A, March 1973.
12. Mady, C.J., Hickey, P.J. and Netzer, D.W., An Investigation of the Combustion Behavior of Solid Fuel Ramjets, Naval Postgraduate School Report Number NPS-67Nt77092, September 1977.

# INITIAL DISTRIBUTION LIST

	No. of Copies
1. Library, Code 0212	2
Dean of Research, Code 012	2
Naval Postgraduate School	
Monterey, CA 93940	
2. Department of Aeronautics	
Code 67	
Naval Postgraduate School	
Monterey, CA 93940	
Prof. M. F. Platzter, Chairman	1
Prof. D. W. Netzer	15
LT. C. A. Stevenson	2
3. Defense Documentation Center	2
Attn: DDC-TCA	
Cameron Station, Bldg. 5	
Alexandria, VA 22314	
4. Naval Air Systems Command	2
Washington, DC 20361	
AIR-330	
5. Naval Weapons Center	
China Lake, CA 93555	
Tech. Library, Code 753	3
F. Zarlingo, Code 3246	3
K. Schadow, Code 388	1
6. Chemical Systems Division	
United Technologies	
P.O. Box 358	
Sunnyvale, CA 94088	
Tech. Library	1
R. Dunlap	1
A. Holzman	1
G. Jensen	1
P. Willoughby	1
P. LaForce	1
7. Chemical Propulsion Information Agency	2
APL-JHU	
Johns Hopkins Road	
Laurel, MD 20810	
8. AFAPL	
Wright-Patterson AFB, OH 45433	
R. R. Craig	1
R. D. Stull	1